

This article was downloaded by:

On: 14 January 2011

Access details: *Access Details: Free Access*

Publisher *Taylor & Francis*

Informa Ltd Registered in England and Wales Registered Number: 1072954 Registered office: Mortimer House, 37-41 Mortimer Street, London W1T 3JH, UK



## Molecular Simulation

Publication details, including instructions for authors and subscription information:

<http://www.informaworld.com/smpp/title~content=t713644482>

### $\text{H}_3\text{O}^+$ and $\text{OH}^-$ in Water

Tamotsu Hashimoto<sup>a</sup>; Yasuaki Hiwatari<sup>b</sup>

<sup>a</sup> Material Structural Formation Process Department, National Industrial Research Institute of Nagoya, Japan <sup>b</sup> Physics Department, Faculty of Science, Kanazawa University, Kanazawa, Japan

**To cite this Article** Hashimoto, Tamotsu and Hiwatari, Yasuaki(1999) ' $\text{H}_3\text{O}^+$  and  $\text{OH}^-$  in Water', *Molecular Simulation*, 21: 4, 239 — 247

**To link to this Article:** DOI: 10.1080/08927029908022064

**URL:** <http://dx.doi.org/10.1080/08927029908022064>

PLEASE SCROLL DOWN FOR ARTICLE

Full terms and conditions of use: <http://www.informaworld.com/terms-and-conditions-of-access.pdf>

This article may be used for research, teaching and private study purposes. Any substantial or systematic reproduction, re-distribution, re-selling, loan or sub-licensing, systematic supply or distribution in any form to anyone is expressly forbidden.

The publisher does not give any warranty express or implied or make any representation that the contents will be complete or accurate or up to date. The accuracy of any instructions, formulae and drug doses should be independently verified with primary sources. The publisher shall not be liable for any loss, actions, claims, proceedings, demand or costs or damages whatsoever or howsoever caused arising directly or indirectly in connection with or arising out of the use of this material.

## $\text{H}_3\text{O}^+$ AND $\text{OH}^-$ IN WATER

TAMOTSU HASHIMOTO<sup>a,\*</sup> and YASUAKI HIWATARI<sup>b</sup>

<sup>a</sup> *Material Structural Formation Process Department, National Industrial  
Research Institute of Nagoya, 462-8510, Japan;*

<sup>b</sup> *Physics Department, Faculty of Science, Kanazawa University,  
Kanazawa, 920-1192, Japan*

(Received May 1998; accepted June 1998)

Using the KKY potential model, we have carried out classical molecular dynamics (MD) simulations of structural and vibrational properties of  $\text{H}_3\text{O}^+$  and  $\text{OH}^-$  in water. We have started simulation from an initial configuration that contains both  $\text{H}_3\text{O}^+$  and  $\text{OH}^-$  simultaneously in a bulk water. As for  $\text{H}_3\text{O}^+$  in water, we have obtained a structure in qualitative agreement with a structure of  $(\text{H}_9\text{O}_4)^+$  predicted previously by *ab initio* calculations. However, the O—O distances between  $\text{H}_3\text{O}^+$  and its coordinated water molecules were larger than the previous *ab initio* calculation. As for  $\text{OH}^-$  in water, we have obtained that around  $\text{OH}^-$  ion, the number of solvated water molecules is larger than in the case of pure water. The O—H stretching vibration frequency of  $\text{H}_3\text{O}^+$  and  $\text{OH}^-$  were shifted to the red and to the blue, respectively, compared to that for  $\text{H}_2\text{O}$ , which is in agreement with the result of *ab initio* MD simulation by Tuckerman *et al.*

**Keywords:** Molecular dynamics simulation; hydronium ion; hydroxyl ion; solvation structure; vibrational frequency shift

### 1. INTRODUCTION

The high proton mobility in water is usually explained by Grotthuss mechanism, namely, a sequence of proton-transfer reactions (proton hopping) between water molecules. However, the detailed mechanism was not clear so far. The proton transfer mechanism in water has been studied theoretically [1–6]. In 1995, by *ab initio* MD simulation, Tuckerman *et al.* studied the structure and dynamics of  $\text{H}_3\text{O}^+$  ion in water and  $\text{OH}^-$  ion in water [2–4]. They reported that in the case of  $\text{H}_3\text{O}^+$  in water, as a proton

---

\*Corresponding author.

moves back and forth along a hydrogen bond, the structure of hydrated  $\text{H}_3\text{O}^+$  changes dynamically between  $(\text{H}_9\text{O}_4)^+$  and  $(\text{H}_5\text{O}_2)^+$ . The transport of a proton is driven by the coordination fluctuations in the first solvation shell water molecules of  $\text{H}_3\text{O}^+$ . They also reported that in the case of  $\text{OH}^-$  ion in water, a planar  $(\text{H}_9\text{O}_5)^-$  complex was formed, and proton transfer occurred only when the complex was transformed to  $(\text{H}_7\text{O}_4)^-$ .

This work aims to study the proton transfer mechanism in water by MD simulation using the KKY potential model [7] to examine whether these mechanisms can be reproduced by a classical molecular dynamics simulations using a dissociable model. In the present study, we have focused our attentions on structural and vibrational properties of a  $\text{H}_3\text{O}^+$  ion and a  $\text{OH}^-$  ion in water.

The KKY potential model represents a system of water with interatomic potential functions: The system consists of oxygen ions and hydrogen ions. They consist of two-body interactions and three-body interactions. The two-body interactions consist of Coulomb interactions, short range repulsions, dispersion potentials, and morse functions representing covalent bonds. The three-body potential function controls the intramolecular H—O—H angles. The fractional charges of hydrogen atoms and oxygen atoms in this model are +0.4 and -0.8, respectively. Using this model, we have previously studied the structural transformations of ice at high pressures [8–10]. In the present paper, we examine the structures and O—H stretching frequency shifts of solvated water ions, which should be compared with experiments and *ab initio* calculations.

## 2. METHOD

We used a model of 64 oxygen atoms and 128 hydrogen atoms with a periodically repeating cubic MD cell. The density of water was chosen to be  $0.997 \text{ g/cm}^3$  corresponding to 300 K and 1 atm [11]. An initial configuration of crystal structure (Ice Ic like structure) was used. Then, we added a hydrogen atom to a water molecule at (0,0,0) and removed a hydrogen atom from a water molecule at  $(L/2, L/2, L/2)$ , where  $L$  is the MD cell length. The distance of  $\text{H}_3\text{O}^+$  and  $\text{OH}^-$  were initially 10.5 Å. The temperature of the system were set to be 400 K during 60000 time steps. During this period, water molecules were not dissociate. Then we scaled the temperature to 300 K for 10000 time steps. We continued the MD simulation keeping the temperature at 300 K using Nosé method [12]. We kept the volume of the system constant throughout the present simulation. After the system was

reached to an equilibrium state, we continued simulation for next 120000 time steps using constant energy algorithm ( $N, V, E$ ), and analyzed various physical quantities using the coordinate data and velocity data during this period. The time step was 0.2 fs. The fifth order Gear predictor-corrector method was used for numerical computation [13] and the Ewald method for Coulomb interactions. The cutoff distance of the two body interactions was 6.2 Å. The cutoff distance of three-body interactions was 3 Å.

### 3. RESULTS

To calculate radial distribution functions of H<sub>3</sub>O<sup>+</sup> and OH<sup>-</sup> in water, we used the coordination data for 120000 time steps, in which, the distance between the oxygens of H<sub>3</sub>O<sup>+</sup> and OH<sup>-</sup> was fluctuated from 4 to 7 Å. Because of this reason, we show radial distribution functions up to 4 Å. This result indicates that the distance between the oxygens of H<sub>3</sub>O<sup>+</sup> and OH<sup>-</sup> is greater or equal to the second neighbor oxygen–oxygen distance in pure water. During this period, proton transfers between water ions and water molecules were not observed.

Figures 1 and 2 show partial radial distribution functions  $g_{O^*O}$ ,  $g_{O^*H}$ , and  $g_{H^*H}$  for both H<sub>3</sub>O<sup>+</sup> and OH<sup>-</sup> in water, where the oxygen atom belonging to H<sub>3</sub>O<sup>+</sup> and OH<sup>-</sup> is denoted by O\* and the hydrogen atom by H\*. For comparison, are shown in the same figures  $g_{OO}$ ,  $g_{OH}$ , and  $g_{HH}$  for pure water. In the case of pure water, the first and the second peak positions of  $g_{OH}$  correspond to the intramolecular O—H distance and the intermolecular O···H distance, respectively. We also show running coordination numbers in the same figures. In the case of pure water, for  $g_{OH}$ , the running coordination number is two at the first peak and about four at the second peak, indicating that about two water molecules donate hydrogen bonds to each water. In  $g_{HH}$ , the first peak corresponds to the intramolecular H—H distance.

In the case of H<sub>3</sub>O<sup>+</sup> in water (Fig. 1), the O—H length is longer and widely distributed than in the case of H<sub>2</sub>O. At the first peak of  $g_{OH}$ , the coordination number is three. There is a small peak (the coordination number at this peak is less than 1) corresponding to the second peak of pure water, indicating that a water molecule sometimes donates a proton to a hydrogen bond with H<sub>3</sub>O<sup>+</sup>. During our simulation, H<sub>3</sub>O<sup>+</sup> always donated protons to hydrogen bonds with coordinated water molecules. From  $g_{OO}$ , we see that the O—O distance between a H<sub>3</sub>O<sup>+</sup> and a water molecule is shorter than that between water molecules in pure water. From  $g_{HH}$ , we see

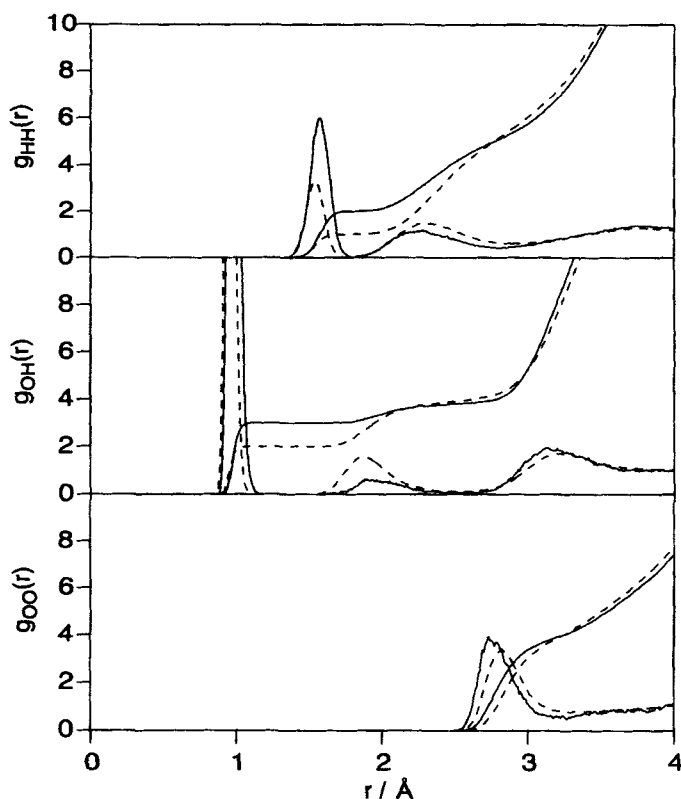


FIGURE 1 Radial distribution functions and running coordination numbers for  $\text{H}_3\text{O}^+$  in water as seen from  $\text{O}^*$  or  $\text{H}^*$  (solid lines) and for pure water (dashed lines).

that the intramolecular  $\text{H}-\text{H}$  distance in  $\text{H}_3\text{O}^+$  is longer than that in pure water due to the nature of a long  $\text{O}^*-\text{H}$  chemical bond distance.

Our results for  $\text{O}-\text{O}$  distance between  $\text{H}_3\text{O}^+$  and water molecules and  $\text{O}-\text{H}$  distance in  $\text{H}_3\text{O}^+$  shows the same trends with *ab initio* MD simulations [2–4] and with *ab initio* calculations of isolated  $(\text{H}_9\text{O}_4)^+$  clusters [14, 16–18]. However, compared with such results, our results for both lengths of  $\text{O}-\text{H}$  and  $\text{O}-\text{O}$  shows that the differences between  $\text{H}_3\text{O}^+$  and pure water were significantly smaller. For pure water, the  $\text{O}-\text{O}$  distance and the  $\text{O}-\text{H}$  distance was 2.84 Å and 0.96 Å, respectively, which were in agreement with experiment [19]. The  $\text{O}-\text{O}$  distance between  $\text{H}_3\text{O}^+$  and water molecules and the  $\text{O}-\text{H}$  distance in  $\text{H}_3\text{O}^+$  were 2.74 Å and 0.98 Å, respectively. The result by Tuckerman *et al.* for the  $\text{O}-\text{O}$  distance

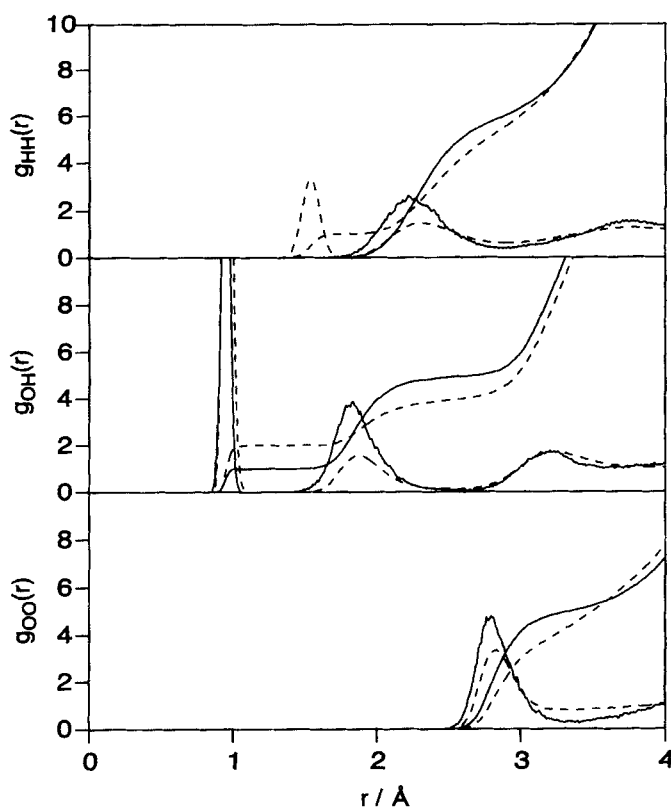


FIGURE 2 Radial distribution functions and running coordination numbers for OH<sup>-</sup> in water as seen from O\* or H\* (solid lines) and for pure water (dashed lines).

is in good agreement with results for isolated cluster calculations (2.6 Å). However, their result for the O—H distance is about 0.1 Å longer than isolated H<sub>9</sub>O<sub>4</sub><sup>+</sup> cluster calculations (1 Å).

In Figure 2, we compared radial distribution functions for OH<sup>-</sup> ion in water with those for pure water. For  $g_{HH}$ , the absence of the peak corresponding to the intramolecular H—H distance of pure water is due to the fact that there is only one H in OH<sup>-</sup> ion. The chemical bonding O\*—H distance for OH<sup>-</sup> ion (0.96 Å) is almost the same as that for pure water (0.96 Å), but its distribution is narrower and shifted to a shorter direction. The hydrogen bonding O\*···H distance (1.84 Å) is smaller than that for pure water (1.88 Å). The O\*—O distance (2.80 Å) is smaller than the oxygen—oxygen distance for pure water (2.84 Å). The running coordination number of H around O\* in the case of OH<sup>-</sup> ion is 1 at the first peak and 4.9 at the

second peak (2.5 Å), while in the case of pure water, the corresponding values were 2 and 3.9, respectively. OH<sup>−</sup> ion is surrounded by about four hydrogen atoms within the hydrogen bond distance of water, which acted as an acceptor of four hydrogen bonds. This indicates a remarkable difference from the case of pure water. The H—O<sup>+</sup>...H angle was about 105 degree for both states, the most energetically favored value for pure water of this potential model. The solvated OH<sup>−</sup> obtained in this calculation corresponds to the (H<sub>9</sub>O<sub>5</sub>)<sup>−</sup> complex observed by Tuckerman *et al.* though it was not a planar complex unlike that they observed.

We did not observe proton transfer during the MD simulation of 120000 time steps (24 ps). Therefore, we could not derive meaningful information about the relationship among hydrogen bonding structures, dynamics of OH<sup>−</sup> and proton diffusion.

We calculated the power spectrum of O—H stretching velocity autocorrelation functions for H<sub>3</sub>O<sup>+</sup> ion, OH<sup>−</sup> ion, and H<sub>2</sub>O in pure water in the same way as used by Tuckerman *et al.* with the following function

$$\tilde{C}_{vv}(\omega) = \frac{1}{n^*} \sum_{i=1}^{n^*} \int dt \langle v_{\text{O}^*\text{H}}^{(i)}(0) v_{\text{O}^*\text{H}}^{(i)}(t) \rangle e^{i\omega t},$$

where the sum runs over the number of O—H bonds, *i.e.*,  $n^* = 3$  for H<sub>3</sub>O<sup>+</sup>, 1 for OH<sup>−</sup>, and the number of hydrogen atoms for pure water, and

$$v_{\text{O}^*\text{H}} = \dot{\mathbf{r}}_{\text{O}^*\text{H}} \cdot \hat{\mathbf{r}}_{\text{O}^*\text{H}},$$

where  $\mathbf{r}_{\text{OH}}$  is the bond vector and  $\hat{\mathbf{r}}_{\text{OH}}$  is the corresponding unit vector. Figure 3 shows the spectra for H<sub>3</sub>O<sup>+</sup>, OH<sup>−</sup>, and H<sub>2</sub>O. The spectrum for H<sub>2</sub>O has a peak at around 3200 cm<sup>−1</sup> corresponding to the intramolecular OH stretching frequency [20]. The frequency for H<sub>3</sub>O<sup>+</sup> is broadly distributed and shifted to a lower frequency direction compared to the result for H<sub>2</sub>O (*i.e.*, by 12% red shift). This trend of the red shift is in agreement with the result by Tuckerman *et al.* (by 17% red shift) and with results by experiments (*e.g.*, shift to 2900 cm<sup>−1</sup> [21]). These frequency shifts are related to the fact that the oxygen–oxygen distance becomes shorter for H<sub>3</sub>O<sup>+</sup> in water than for pure water [22] as shown in Figure 1. We have carried out the same calculation for OH<sup>−</sup>. The peak of the spectrum for OH<sup>−</sup> is sharper than that for H<sub>2</sub>O and shifted only by 6% to a higher frequency direction. This frequency shift is slightly larger than the result by Tuckerman *et al.* (4% blue shift).

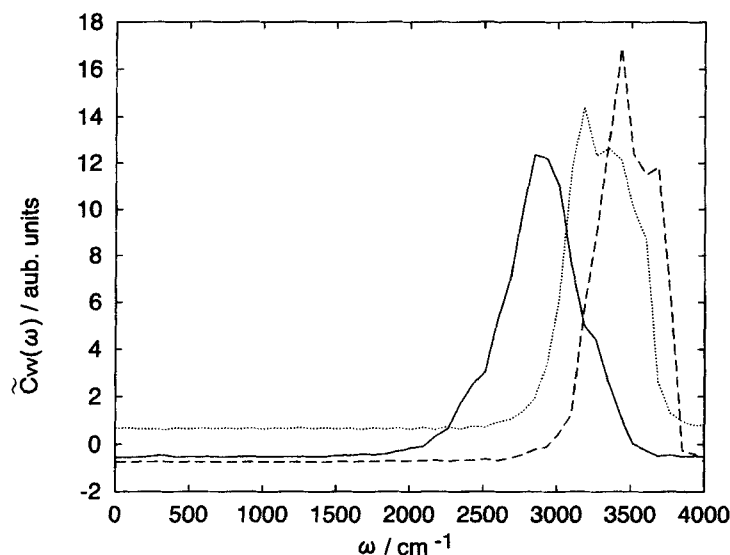


FIGURE 3 Power spectra of O—H bond velocity autocorrelation functions for H<sub>3</sub>O<sup>+</sup> in water (solid line), OH<sup>-</sup> in water (dashed line), and pure water (dotted line).

#### 4. CONCLUSION

Using a dissociable model of water (the KKY potential model), we studied structural and vibrational properties of H<sub>3</sub>O<sup>+</sup> and OH<sup>-</sup> in a bulk water. As to H<sub>3</sub>O<sup>+</sup> ion in water, we obtained the following results. (1) The distance between the oxygen atoms of H<sub>3</sub>O<sup>+</sup> and a water molecule which is hydrogen bonding to H<sub>3</sub>O<sup>+</sup> is shorter than the oxygen–oxygen distance in pure water. The O—H distance in H<sub>3</sub>O<sup>+</sup> ion is longer compared to that in H<sub>2</sub>O. These results are in qualitative agreement with results obtained by *ab initio* calculations. (2) The peak of the power spectrum of the velocity autocorrelation function of O—H stretching vibration for H<sub>3</sub>O<sup>+</sup> is shifted to a lower frequency compared to that of H<sub>2</sub>O. This trend is in agreement with the IR spectrum study of H<sub>3</sub>O<sup>+</sup> in water and also in agreement with *ab initio* MD simulation of Tuckerman *et al.*

As to the OH<sup>-</sup> ion in water, we obtained the following results. (1) The O—H distance in OH<sup>-</sup> ion is the same as that for H<sub>2</sub>O. However, the distribution of O—H distance for OH<sup>-</sup> ion is shifted to a shorter direction compared to that for H<sub>2</sub>O. The (H<sub>9</sub>O<sub>5</sub>)<sup>-</sup> structure was not planar unlike the result by Tuckerman *et al.* (2) The peak of the power spectrum of the velocity autocorrelation function of O—H stretching vibration for OH<sup>-</sup> ion



is slightly shifted to a higher frequency compared to that for  $\text{H}_2\text{O}$  in agreement with the result by Tuckerman *et al.*

From these results, we conclude that the KKY potential model can partly represent the structures and vibrational properties of  $\text{H}_3\text{O}^+$  ion and  $\text{OH}^-$  ion in water. The lifetime of hydronium ion is about 1 ps [20]. However, during our MD simulation of 120000 time steps (24 ps), proton transfer was not observed. In the proton transfer process, tunneling of a proton through a potential barrier may be more important [5] in water under investigation. However, by improving potential parameters of the present model which leads, for example, to reproduce the  $\text{O}^*-\text{O}$  distance more properly, proton transfer may take place through classical hopping mechanisms.

### References

- [1] Agmon, N. (1995). "The Grotthuss mechanism", *Chem. Phys. Lett.*, **244**, 456.
- [2] Tuckerman, M., Laasonen, K., Sprik, M. and Parrinello, M. (1994). "Ab initio simulations of water and water ions", *J. Phys. Cond. Matt.*, **6**, A93.
- [3] Tuckerman, M., Laasonen, K., Sprik, M. and Parrinello, M. (1995). "Ab initio molecular dynamics simulation of solvation and transport of  $\text{H}_3\text{O}^+$  and  $\text{OH}^-$  ions in water", *J. Phys. Chem.*, **99**, 5749.
- [4] Tuckerman, M., Laasonen, K., Sprik, M. and Parrinello, M. (1995). "Ab initio molecular dynamics simulation of the solvation and transport of hydronium and hydroxyl ions in water", *J. Chem. Phys.*, **103**, 150.
- [5] Lobaugh, J. and Voth, G. A. (1996). "The quantum dynamics of an excess proton in water", *J. Chem. Phys.*, **104**, 2056.
- [6] Kobayashi, C., Iwahashi, K., Saito, S. and Ohmine, I. (1996). "Dynamics of proton attachment to water cluster: Proton transfer, evaporation, and relaxation", *J. Chem. Phys.*, **105**, 6358.
- [7] Kumagai, N., Kawamura, K. and Yokokawa, T. (1994). "An interatomic potential model for  $\text{H}_2\text{O}$ : Applications to water and ice polymorphs", *Mole. Simul.*, **12**, 177.
- [8] Hashimoto, T., Sugawara, S. and Hiwatari, Y. (1996). "Structural transformations of ice at high pressures via molecular dynamics simulations", *Mole. Simul.*, **18**, 115.
- [9] Hashimoto, T., Oda, T. and Hiwatari, Y. (1997). "Structural transformations of ice at high pressures via molecular dynamics simulations II", *Mole. Simul.*, **18**, 395.
- [10] Hashimoto, T., Sugawara, S. and Hiwatari, Y. (1997). "Structural transformations of ice at normal and high pressures via molecular dynamics simulations", *J. Phys. Chem.*, **B101**, 6293.
- [11] Kell, G. S. (1975). "Density, Thermal Expansivity, and Compressibility of Liquid Water from 0°C to 150°C: Correlations and Tables for Atmospheric Pressure and Saturation Reviewed and Expressed on 1968 Temperature Scale", *J. Chem. Eng. Dat.*, **20**, 97.
- [12] Nosé, S. (1984). "A unified formulation of the constant temperature molecular dynamics methods", *J. Chem. Phys.*, **81**, 511.
- [13] van Gunsteren, W. F. and Berendsen, H. J. C. (1977). "Algorithms for macromolecular dynamics and constraint dynamics", *Mole. Phys.*, **34**, 1311.
- [14] Remington, R. and Schaefer, H. F. (unpublished results), quoted in Ref. [15].
- [15] Yeh, L. I., Okumura, M., Myers, J. D., Price, J. M. and Lee, Y. T. (1989). "Vibrational spectroscopy of the hydrated hydronium cluster ions  $\text{H}_3\text{O}^+ \cdot (\text{H}_2\text{O})_n$  ( $n = 1, 2, 3$ )", *J. Chem. Phys.*, **91**, 7319.
- [16] Wei, D. and Salahub, D. R. (1994). "Hydrated proton clusters and solvent effects on the proton transfer barrier: A density functional study", *J. Chem. Phys.*, **101**, 7633.

- [17] Newton, M. D. and Ehrenson, S. (1971). "Ab initio studies on the structures and energetics of inner- and outer-shell hydrates of the proton and the hydroxide ion", *J. Am. Chem. Soc.*, **93**, 4971.
- [18] Newton, M. D. (1978). "Ab initio studies of hydrated H<sub>3</sub>O<sup>+</sup> ion. II. The energetics of proton motion in higher hydrates ( $n = 3-5$ )", *J. Chem. Phys.*, **67**, 5535.
- [19] Soper, A. K. and Philips, M. G. (1986). "A new determination of the structure of water at 25°C", *Chem. Phys.*, **107**, 47.
- [20] Eisenberg, D. and Kauzmann, W. *The Structure and Properties of Water* (Oxford University Press, New York, 1969), Chap. 4.
- [21] Giguère, P. A. and Turrell, S. (1976). "H<sub>3</sub>O<sup>+</sup> ions in aqueous acid solutions. The infrared spectra revisited", *Can. J. Chem.*, **54**, 3477.
- [22] Bratos, S., Ratajczak, H. and Viot, P. "Properties of h-bonding in the infrared spectral range", In: *Hydrogen-Bonded Liquids*, Dore, J. C. and Texeira, J. (Eds.) (Kluwer, Dordrecht, 1991).